Water adsorption on the α-Al_2O_3(0001) surface

P. Thissen and G. Grundmeier
Lehrstuhl für Technische und Makromolekulare Chemie, Universität Paderborn, 33098 Paderborn, Germany

S. Wippermann and W. G. Schmidt
Lehrstuhl für Theoretische Physik, Universität Paderborn, 33098 Paderborn, Germany

(Received 2 April 2009; revised manuscript received 4 November 2009; published 3 December 2009)

The adsorption of water monomers, small water clusters, and water thin films on α-Al_2O_3(0001) surfaces is studied by density-functional theory. For the metal-terminated surface, the calculations favor the dissociative adsorption for low coverages and the formation of hexagons of alternating dissociatively and molecularly adsorbed water monomers for water-rich conditions. The calculated adsorption energy per water molecule decreases from about 1.5 eV for single adsorbed molecules to about 1.2 eV for thin films in very good agreement with our temperature programmed desorption experiments. The fully hydroxylated (gibbsitelike) surface, however, represents the thermodynamic ground state of the α-Al_2O_3(0001) surface in the presence of water.

DOI: 10.1103/PhysRevB.80.245403 PACS number(s): 68.43.Bc, 82.30.Rs

I. INTRODUCTION

The interaction of water with solid surfaces is fundamental to research in various fields ranging from atmospheric chemistry to corrosion and heterogeneous catalysis. Despite substantial research efforts, however, precise information on the water geometry at the atomic level often seems elusive for the ubiquitous liquid phase[1,2] as well as for many cases of substrate-supported thin water films and clusters prepared in the laboratory.[3–9]

The interaction of water with aluminum oxide has found interest because of the extensive use if this material, e.g., as a catalyst as well as a catalyst support, and by its role in environmental chemistry. Moreover, the well-defined Al-terminated α-Al_2O_3(0001) surface is a widely studied model for water interaction with metal-oxide surfaces. Experimentally, most studies propose water dissociation on the Al-terminated α-Al_2O_3(0001) surface. This was concluded from high-resolution electron-energy-loss spectroscopy (HREELS) studies[10] as well as thermal desorption experiments (TDS).[11,12] X-ray photoemission experiments[13] were interpreted to indicate water dissociation in particular at surface defect sites. Early ultraviolet photoelectron spectra, on the other hand, seem to indicate molecular adsorption of water at room temperature.[14] Also the mobility of the adsorbed molecules on the α-Al_2O_3(0001) surface seems to be a somewhat open question. In Ref. 12 a low mobility of the hydroxyl groups at the surface was stated in contrast to the interpretation of dynamic scanning force microscopy images of the water exposed α-Al_2O_3(0001) surface.[15] Theoretically, most *ab initio* studies agree on the stability of the dissociative vs the molecular adsorption[16–18] while one cluster study[19] found little difference between the energies of molecular and dissociative adsorption of water. A recent density-functional theory (DFT) study compares the energetics of a wide range of adsorption geometries for various coverages.[20] However, this comparison does not include the possibility of a dissociative adsorption as concluded from many experimental studies. Also, the change in the surface composition upon adsorption is not considered in these studies despite early indications for the high stability of the oxygen-terminated surface in the presence of water.[17,21,22] This is confirmed in a very recent study by Ranea *et al.*[23] that finds the fully hydroxylated surface to be the thermodynamic ground state in the presence of water, but concluded that the actual surface composition will depend strongly on the sample history.

Here we explore the energetics of both molecularly and dissociatively adsorbed water for various coverages by DFT calculations. Potential energy surfaces for surface adsorbed water molecules, hydrogen, and hydroxyl groups are presented to address the controversial issue of surface mobility. In addition, the adsorption energetics is addressed by temperature programmed desorption (TPD) spectroscopy.

II. THEORY

The calculations are performed using DFT within the generalized gradient approach (GGA) as implemented in the vienna *ab initio* simulation package (VASP).[24] The electron-ion interaction is described by the projector-augmented wave scheme.[25] The electronic wave functions are expanded into plane waves up to a kinetic energy of 360 eV. The surface is modeled by periodically repeated slabs. Each supercell consists of 18 atomic layers within (2×2) periodicity plus the adsorbed water and a vacuum region equivalent to 18 Å. The 15 uppermost layers as well as the adsorbate degrees of freedom are allowed to relax until the forces on the atoms are below 20 meV/Å. The Brillouin zone integration is performed using $2\times2\times1$ Monkhorst-Pack meshes. We use the PW91 functional[26] to describe the electron exchange and correlation energy within the GGA. It describes the hydrogen bonds in solid water (ice Ih) in good agreement with experiment.[27,28]

III. EXPERIMENTAL

Experimentally, after cleaning with concentrated phosphoric acid (85%), rinsing with water, and drying in a stream

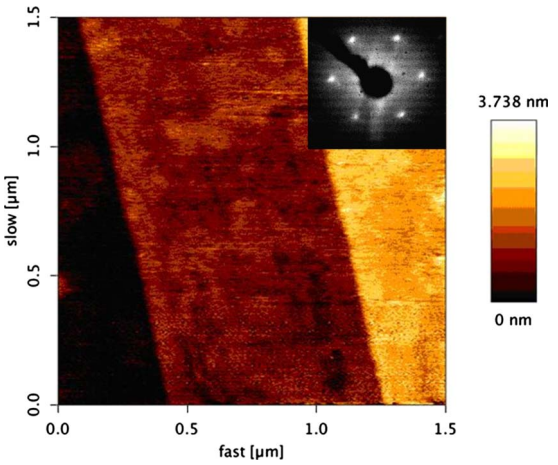

FIG. 1. (Color online) AFM topography of the single crystalline α-$Al_2O_3(0001)$ surface. Step heights are typically about 1 nm. The inset shows LEED pattern recorded at 60 eV representing the hexagonal symmetry of the surface.

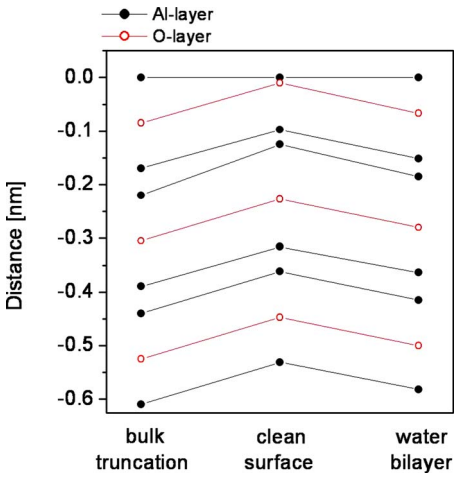

FIG. 2. (Color online) Schematic side view of the bulk and slab state indicating the vertical surface relaxation of Al (solid) and O (dashed) layers. The zero line corresponds to the respective outermost surface atom.

of nitrogen, the sapphire crystal was annealed in air in a high-purity furnace at about 1600 K for 24 h. The annealing produced a surface with large terraces (>1 μm) as evidenced by atomic force microscopy (AFM) and low-energy electron diffraction (LEED); cf. Fig. 1. The ultrahigh vacuum (UHV) system consists of a pumping system and the vacuum vessel. Vacuum was maintained by two turbo molecular pumps backed by a rotary oil pump. The sample manipulator is based on a rotatable rod that can be moved horizontally and screws allow the accurate positioning of the sample. The manipulator also has electrical feedthroughs with ceramic insulation for connecting the sample to a power supply for resistive heating and two thermocouple wires to a temperature controller. Temperatures of up to approximately 1000 K can thus be obtained at the single crystal sample. The heating power is regulated by a temperature controller that reads the voltage of a thermocouple welded to the side of the sample. The different surface coverages of water were achieved just before transferring the sample to UHV. One sapphire sample was taken fresh from the furnace (movement time through ambient air until UHV transfer about 2 min). The second sample was put into liquid water for 1 min and the last one was activated in low-temperature water plasma for the same time. The TPD experiments were driven with a heating rate β of 1 K s^{-1}.

IV. RESULTS AND DISCUSSION

While the corundum structure of bulk α-Al_2O_3 has a rhombohedral symmetry, the atomic positions are usually given in terms of a hexagonal unit cell. The Al-terminated α-$Al_2O_3(0001)$ surface has $p3$ symmetry, i.e., a threefold rotational axis through the Al ions and no mirror planes. In good agreement with previous studies,[29,30] we find upon structural relaxation of the clean surface that the outermost Al ions move toward the bulk ending up almost in plane with the O atoms; cf. Fig. 2.

We start the adsorption study by determining the potential energy surfaces (PES) for (a) single water monomers, (b) hydrogens in the presence of a surface adsorbed hydroxyl group, and (c) hydroxyl groups in the presence of a surface adsorbed hydrogen on the clean Al-terminated α-$Al_2O_3(0001)$ surface, respectively. Apart from the lateral position of one adsorbate atom, the structural degrees of freedom of both substrate and adsorbate were fully relaxed in these calculations. The calculated data are shown in Fig. 3. In order to account for the fact that energy barriers hinder the free rotation of surface adsorbed water molecules, the minimum energy geometry for every PES sampling point was obtained by probing different molecular starting orientations. As can be seen in Fig. 3, the energy landscape experienced by molecularly adsorbed water monomers as well as dissociated hydrogens or hydroxyl groups is rather corrugated, with maximum energy differences/minimum diffusion energy barriers of 0.54/0.48, 1.54/0.66, and 1.54/1.31 eV. These data clearly support the view of a rather low mobility, in particular of the hydroxyl groups, at the surface.[12] The diffusion barriers for water monomers are somewhat lower but still substantial.

Starting from the low-energy adsorption configuration of single water monomers on the (2×2) surface unit cell, the water coverage was systematically increased to eight molecules. The corresponding lowest-energy structures for the respective coverage on the Al-terminated surface are denoted by ATn in the following, where n corresponds to the number of molecules per (2×2) surface unit cell. Among others, the adsorption configurations from Ref. 20 as well as (partially) dissociated adsorption models were probed. In addition, we calculate the energetics of the fully hydroxylated (gibbsite-like) surface that can be understood as the triple hydrogenation of the nonstoichiometric O-terminated α-$Al_2O_3(0001)$ surface.[23,31] It is denoted as FH in the following. The structures resulting from the adsorption (removal) of n water monomers on top of (from) this structure are denoted as FH$(-)n$.

In order to compare adsorption models with different water coverages, the thermodynamic grand-canonical potential

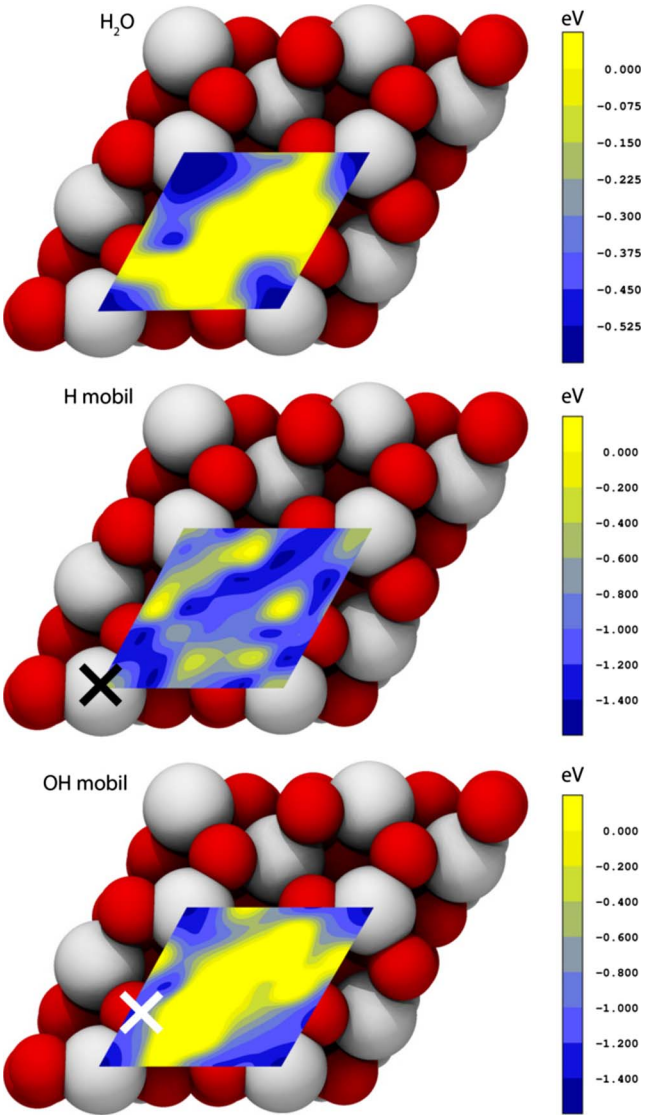

FIG. 3. (Color online) Potential energy surfaces for (a) single water monomers, (b) hydrogens in the presence of OH groups (black cross), and (c) hydroxyl groups in the presence of H (white cross) on the α-$Al_2O_3(0001)$ surface, respectively.

$$\Omega(\mu^{H_2O}) = F_{surf}(n) - n\mu^{H_2O} \approx E_{surf}(n) - n\mu^{H_2O} \qquad (1)$$

needs to be calculated,[32] where $F_{surf}(n)$ is the surface free energy which we approximate by the total surface energy $E_{surf}(n)$ at zero temperature assuming similar entropy contributions for different adsorption configurations. The number of adsorbate molecules is represented by n. Figure 4 shows the resulting phase diagram in dependence on the water chemical potential μ^{H_2O}. Here two important values are indicated. Extreme water-rich conditions are marked by a vertical line denoted μ_{solid}. This value corresponds to a Al_2O_3 surface in equilibrium with bulk water approximated here by calculations for ice Ih.[28] Lower values of μ indicate an increasingly dry environment. The zero-temperature calculation for gas-phase water molecules is indicated by another vertical line. At finite temperatures, entropy corrections will lower the respective value of μ for the surface in equilibrium

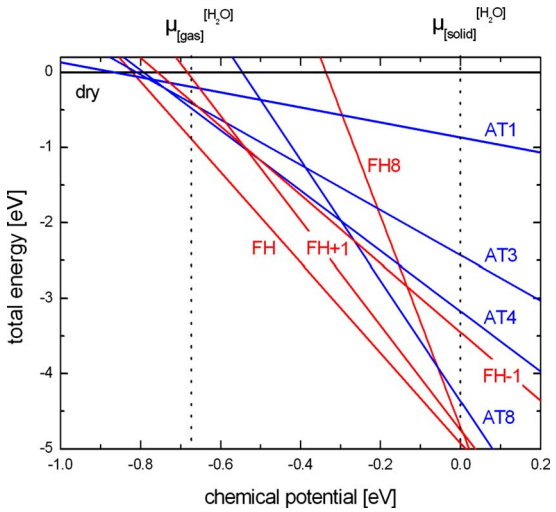

FIG. 4. (Color online) Calculated phase diagram of the α-$Al_2O_3(0001)$ surface in dependence on the water chemical potential $\Delta\mu$ given with respect to ice Ih.

with a reservoir of water vapor[33] and also slightly affect the relative stability of different surface phases; see, e.g., Refs. 31, 34, and 35. The inclusion of the fully hydroxylated surfaces[23] in the phase diagram seemingly introduces an additional degree of freedom: the stability of these structures will depend on the chemical potential of the surface liberated Al. It may, for example, diffuse into the bulk material or desorb as $Al(OH)_3$, while the remaining protons of the water molecules adsorb on the three O subsurface atoms that were originally bonded to the now released Al atom. From a thermodynamic perspective, the Al atoms are in any case in equilibrium with bulk Al_2O_3, even if the particle exchange with the bulk material is kinetically hindered and may be slow.

As expected, the clean Al_2O_3 surface is stable for low values of the water chemical potential. As the environment gets more and more humid, a variety of water-adsorbed surface structures may be observed. Considering first the adsorption on the Al-terminated surface, the adsorption models AT1 and AT3 are stable for a very small window of preparation conditions, while the full monolayer (AT4) and the bilayer (AT8) structure are stable for a relatively wide range of water-rich and extreme water-rich conditions. This sequence, however, does not correspond to the thermodynamic ground state of the surface that is characterized by the fully hydroxylated surface. Its stability reflects the strength of the H-OAl bond and is consistent with the negative heat of formation of the α-$Al_2O_3 + 3H_2O \leftrightarrow 2Al(OH)_3$ reaction at ambient conditions. As pointed out already in Ref. 23, however, the formation of the FH structures is expected to be kinetically hindered and the actual surface phase will strongly depend on the sample history. The removal of water monomers from the fully hydroxylated surface is even less favored than the adsorption of additional water molecules on top of the FH structure.

Low coordination of surface Al ions on clean α-$Al_2O_3(0001)$ makes these sites strong Lewis acids, i.e., electron acceptors, which readily adsorb molecules such as H_2O, that can add electron density. The dissociative adsorp-

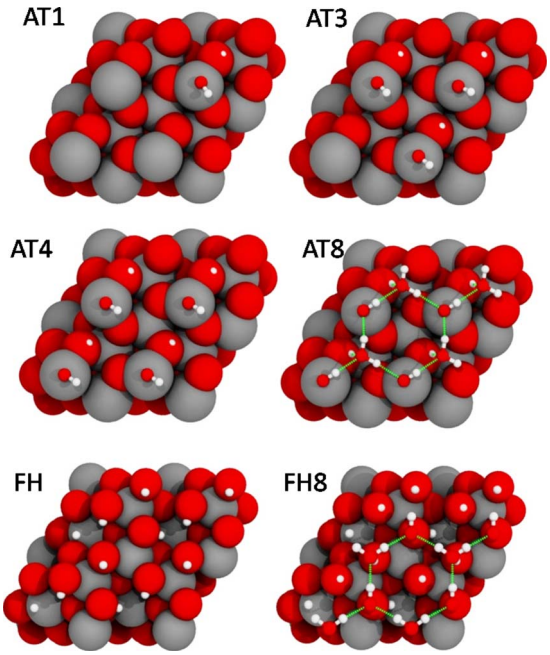

FIG. 5. (Color online) Schematic top view of relevant adsorption structures.

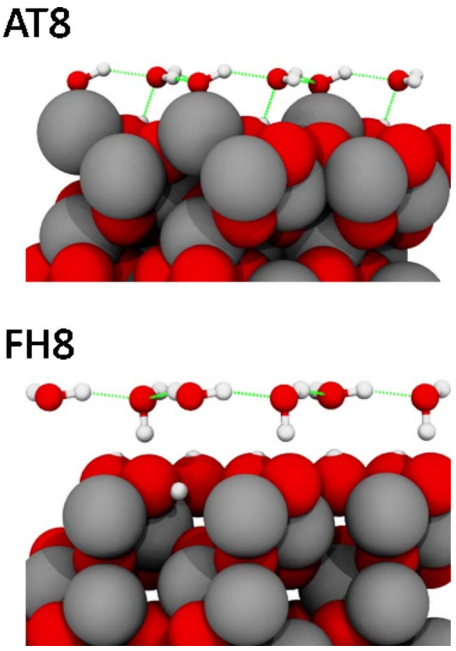

FIG. 6. (Color online) Schematic side view of a water bilayer adsorbed on the Al-terminated (AT8) or fully hydroxylated (FH8) surface.

tion is primarily heterolytic in nature. Adsorbed H_2O dissociating can be viewed as splitting into H^+ and OH^-, with the proton transferred to a nearby surface site in a 1–4 mechanism.[16] For all coverages, adsorption of H_2O significantly disrupts the clean α-Al_2O_3(0001) surface geometry. The adsorption pulls the surface Al out of its relaxed surface position and elongates its three bonds to neighboring oxygen ions. The bonds between this Al and second-layer O are significantly longer and they are elongated even beyond the bulk values; cf. Fig. 2. That single H_2O molecules prefer to adsorb dissociatively on α-Al_2O_3(0001), even in the absence of defects, differs from the behavior predicted in an earlier study of H_2O on MgO(100).[36] In that case, dissociative adsorption was favored in the vicinity of a step, but molecular adsorption was more stable on the ideal surface.

The most relevant structures from the surface phase diagram are shown in Figs. 5 and 6. For low water coverages on Al-terminated surfaces, single dissociated molecules (AT1) are stable. The ground-state geometry calculated here corresponds to the 1–2 geometry discussed in Ref. 16. It is energetically nearly degenerate with the 1–4 structure. The latter structure, however, requires a substantially lower activation energy of only 0.09 eV.[16] If all surface Al atoms are occupied by hydroxyl groups, additional water molecules do not dissociate but form hydrogen bonds with the preadsorbed H and OH groups; see Fig. 6. Hexagons form (AT8) that are somewhat reminiscent of the water hexagons formed on many metal surfaces.[6,9] In contrast to the latter, however, the hexagon structures formed on α-Al_2O_3(0001) consist of alternating dissociated and intact molecules, which might explain some of the experimental ambiguities discussed above. It is interesting to note that a recent theoretical study by Scheffler and co-workers found similarly a crossover to a mixed molecular and dissociative adsorption mode with increasing water chemical potential for water adsorption on Fe_3O_4(0001).[37] Also shown in Figs. 5 and 6 are the fully hydroxylated surface (FH) and the adsorption of an additional water bilayer on top (FH8).

Figure 7 shows the adsorption energy per molecule calculated as

$$E_{\text{ads}} = \frac{(E_n - E_0) - nE_{\text{H}_2\text{O}}}{n}. \tag{2}$$

We find the relative adsorption energy to vary only moderately between the different adsorption geometries. This indicates that the surface-molecule interaction is dominant over the molecule-molecule interaction. A closer look at the adsorption energies shows two additional trends: a slight decrease in the adsorption energy with increasing coverage of dissociated molecules is followed by a somewhat more pro-

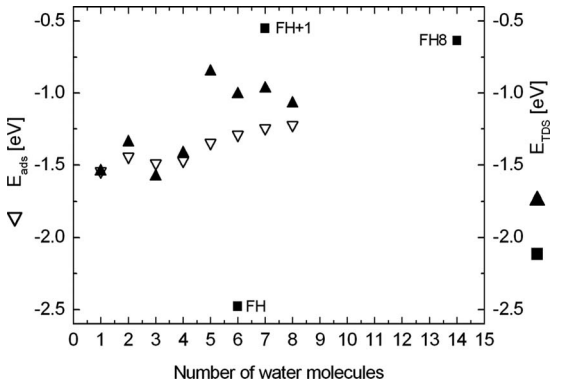

FIG. 7. Calculated adsorption energy per water molecule for the adsorption configurations AT1–AT8 as well as FH, FH1, and FH8 models.

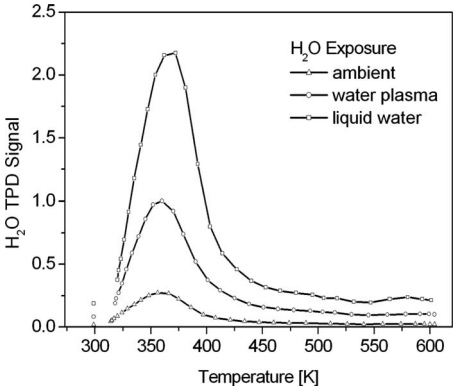

FIG. 8. TPD spectra of H_2O from the α-Al_2O_3(0001) surface recorded after various H_2O exposures at 298 K. The heating rate was 1 K s^{-1}.

nounced decrease as soon as the molecular adsorption starts for coverages above one water molecule per primitive surface unit cell (AT4). Overall we find a variation between about 1.5 and 1.2 eV for the adsorption energy. The lower limit agrees well with the calculations of Ranea *et al.*[20] who considered exclusively molecularly adsorbed water. Also the energy difference between molecularly and dissociatively adsorbed water is close to the earlier calculations which state about 0.43 eV for the low-coverage regime.[16]

Also shown in Fig. 7 are the differential binding energies E_{TDS} calculated as

$$E_{\mathrm{TDS}} = E_n - E_{n-1} - E_{\mathrm{H_2O}}. \tag{3}$$

Here we calculated a somewhat larger spread between 0.8 and 1.6 eV for adsorption on the Al-terminated surface. This spread gets even larger if the energy is considered to either extract one water monomer from the FH structure (about 2.5 eV) or to remove water monomers adsorbed on top of the fully hydroxylated surface (about 0.6 eV); see square symbols in Fig. 7. Water adsorption in excess of one monolayer leads to a decrease in the adsorption energy that is even more pronounced for the fully hydroxylated surface than in case of adsorption on the metal-terminated surface; see Ref. 34.

The adsorption energetics was also studied using TPD measurements of differently water-treated α-Al_2O_3(0001) surfaces. Figure 8 demonstrates that H_2O desorbs over a temperature range from 300 to 450 K. The thermal desorption feature is dominated by a well-defined main peak centered around 350 K. In order to extract desorption kinetic parameters, a Redhead-based analysis has been applied to the desorption threshold region.[38] By assuming a preexponential factor of 10^{13} s^{-1} and using the Redhead equation with the heating rate β=1 K s^{-1} (determined from the differential of the experimental heating curve of the sample at the peak temperatures), energies of 0.9–1.5 eV for the desorption peak were determined. This is in very good agreement with the calculated differential binding energies of 0.8–1.6 eV for the AT adsorption models and close to earlier TDS work that reported a range of 1.0–1.8 eV.[12] We cannot completely exclude surface defects such as step edges[39,40] to contribute additionally to the broadening of the TPD peak. The excellent (1×1) LEED pattern as well as our AFM data, cf. Fig. 1, indicates, though, that surface defects are less important than different water bonding situations for the broadening of the TPD peak.

The measured range of desorption temperatures corresponds to the variation in desorption energies calculated for dissociatively and molecularly adsorbed water on the metal-terminated Al_2O_3 surface. The adsorption energies concluded from the TPD experiments are clearly not compatible with the calculations for the FH models. While the removal of a water molecule from the FH surface requires an energy of about 2.5 eV, excess water on top of the FH structure bonds very weakly with adsorption energies only slightly larger than 0.5 eV. These values are outside the range of 0.9–1.5 eV of the measured desorption peak.

V. CONCLUSIONS

To summarize, DFT-GGA calculations as well as TPD spectroscopy for water adsorbed on the clean α-Al_2O_3(0001) surface were performed. For low water coverages single dissociated water molecules are energetically most favored on the Al-terminated surface. The PES for both intact water molecules as well as water fragments adsorbed on α-Al_2O_3(0001) is highly corrugated indicating a low surface mobility. Increasing the water coverage on the Al-terminated surface favors complex structures consisting of both dissociated and intact water monomers. The corresponding variation in the adsorption energy per atom is in good accord with our TPD data. The thermodynamic ground state of the surface is fully hydrogenated. The corresponding adsorption energies, however, are either too large (fully hydroxylated surface) or too low (adsorption on top of the fully hydroxylated surface) to account for the TPD data. We therefore conclude that the adsorption kinetics is very important for the actual surface composition and that short water exposure times are not sufficient to form the fully hydroxylated surface.

ACKNOWLEDGMENTS

Financial support from the DFG as well as grants of supercomputer time by the Höchstleistungs-Rechenzentrum Stuttgart and the Paderborn Center for Parallel Computing PC^2 are gratefully acknowledged.

[1] P. Wernet, D. Nordlund, U. Bergmann, M. Cavalleri, M. Odelius, H. Ogasawara, L. Å. Naäslund, T. K. Hirsch, L. Ojamäe, P. Glatzel, L. G. M. Pettersson, and A. Nilsson, Science **304**, 995 (2004).
[2] A. Hermann, W. G. Schmidt, and P. Schwerdtfeger, Phys. Rev. Lett. **100**, 207403 (2008).
[3] M. Henderson, Surf. Sci. Rep. **46**, 1 (2002).
[4] P. J. Feibelman, Science **295**, 99 (2002).
[5] P. J. Feibelman, Phys. Rev. Lett. **90**, 186103 (2003).
[6] A. Michaelides and K. Morgenstern, Nature Mater. **6**, 597 (2007).
[7] J. Stähler, M. Mehlhorn, U. Bovensiepen, M. Meyer, D. O. Kusmierek, K. Morgenstern, and M. Wolf, Phys. Rev. Lett. **98**, 206105 (2007).
[8] F. Traeger, D. Langenberg, Y. K. Gao, and Ch. Wöll, Phys. Rev. B **76**, 033410 (2007).
[9] S. Wippermann and W. G. Schmidt, Phys. Rev. B **78**, 235439 (2008).
[10] V. Coustet and J. Jupille, Surf. Sci. **307-309**, 1161 (1994).
[11] J. W. Elam, C. E. Nelson, M. A. Cameron, M. A. Tolbert, and S. M. George, J. Phys. Chem. B **102**, 7008 (1998).
[12] C. E. Nelson, J. W. Elam, M. A. Cameron, M. A. Tolbert, and S. M. George, Surf. Sci. **416**, 341 (1998).
[13] P. Liu, T. Kendelewicz, G. E. Brown, E. J. Nelson, and S. A. Chambers, Surf. Sci. **417**, 53 (1998).
[14] D. B. Almy, D. C. Foyt, and J. M. White, J. Electron Spectrosc. Relat. Phenom. **11**, 129 (1977).
[15] C. Barth and M. Reichling, Nature (London) **414**, 54 (2001).
[16] K. C. Hass, Science **282**, 265 (1998).
[17] R. Di Felice and J. E. Northrup, Phys. Rev. B **60**, R16287 (1999).
[18] V. Shapovalov and T. N. Truong, J. Phys. Chem. B **104**, 9859 (2000).
[19] J. M. Wittbrodt, W. L. Hase, and H. B. Schlegel, J. Phys. Chem. B **102**, 6539 (1998).
[20] V. Ranea, W. Schneider, and I. Carmichael, Surf. Sci. **602**, 268 (2008).
[21] P. D. Tepesch and A. A. Quong, Phys. Status Solidi B **217**, 377 (2000).
[22] X.-G. Wang, A. Chaka, and M. Scheffler, Phys. Rev. Lett. **84**, 3650 (2000).
[23] V. Ranea, I. Carmichael, and W. Schneider, J. Phys. Chem. C **113**, 2149 (2009).
[24] G. Kresse and J. Furthmüller, Comput. Mater. Sci. **6**, 15 (1996).
[25] G. Kresse and D. Joubert, Phys. Rev. B **59**, 1758 (1999).
[26] J. P. Perdew, J. A. Chevary, S. H. Vosko, K. A. Jackson, M. R. Pederson, D. J. Singh, and C. Fiolhais, Phys. Rev. B **46**, 6671 (1992).
[27] D. R. Hamann, Phys. Rev. B **55**, R10157 (1997).
[28] C. Thierfelder, A. Hermann, P. Schwerdtfeger, and W. G. Schmidt, Phys. Rev. B **74**, 045422 (2006).
[29] I. Batyrev, A. Alavi, and M. W. Finnis, Faraday Discuss. **114**, 33 (1999).
[30] M. Causa, R. Dovesi, C. Pisani, and C. Roetti, Surf. Sci. **215**, 259 (1989).
[31] A. Marmier and S. C. Parker, Phys. Rev. B **69**, 115409 (2004).
[32] G.-X. Qian, R. M. Martin, and D. J. Chadi, Phys. Rev. Lett. **60**, 1962 (1988).
[33] B. Lange and W. Schmidt, Surf. Sci. **602**, 1207 (2008).
[34] Z. Łodziana, J. K. Nørskov, and P. Stoltze, J. Chem. Phys. **118**, 11179 (2003).
[35] M. Valtiner, M. Todorova, G. Grundmeier, and J. Neugebauer, Phys. Rev. Lett. **103**, 065502 (2009).
[36] M. J. Stirniman, C. Huang, R. S. Smith, S. A. Joyce, and B. D. Kay, J. Chem. Phys. **105**, 1295 (1996).
[37] N. Mulakaluri, R. Pentcheva, M. Wieland, W. Moritz, and M. Scheffler, Verhandl. DPG **44**, 465 (2009); Phys. Rev. Lett. **103**, 176102 (2009).
[38] P. A. Redhead, Vacuum **12**, 203 (1962).
[39] R. C. Barrett and C. F. Quate, J. Vac. Sci. Technol. A **8**, 400 (1990).
[40] V. E. Heinrich and P. A. Cox, *The Surface Science of Metal Oxides* (Press Syndicate of the University of Cambridge, Cambridge, 1994).